J|A|C|S
ARTICLES
Published on Web 05/26/2006

# Helix Triangle: Unique Peptide-Based Molecular Architecture

Kentaro Yoshida, Shin-ichi Kawamura, Tomoyuki Morita, and Shunsaku Kimura*

*Contribution from the Department of Material Chemistry, Graduate School of Engineering, Kyoto University, Kyoto-Daigaku-Katsura, Nishikyo-ku, Kyoto 615-8510, Japan*

Received April 3, 2006; E-mail: shun@scl.kyoto-u.ac.jp

***Abstract:*** We here report a unique cyclic peptide structure, "helix triangle", as a unique example of peptide-based molecular architecture. The cyclic peptide is designed to have a triangular shape in which three 9mer helical peptide units make the sides and three pyrene derivatives make the apexes. The helical peptide units are ideally linear, and the pyrene units are ideal 60° angular components. The yield of the cyclic peptide was relatively high despite its large cycle size. Absorption and fluorescence spectroscopy revealed that the three pyrene units do not interact with each other electronically, and circular dichroism spectroscopy indicated that the helical peptide units take $3_{10}$-helical conformation. Geometry optimization by the semi-empirical molecular orbital method gave a triangular structure with $3_{10}$-helices as the plausible molecular structure. To gain more information on the geometry and demonstrate one example of its self-assemblies, the monolayer of the cyclic peptide was prepared at the air/water interface, and its surface pressure-molecular area isotherm was studied. The isotherm indicated formation of a stable monolayer and suggested that the cyclic peptide actually takes the triangular structure predicted by the geometry optimization. The monolayer was then transferred onto a substrate and characterized by various methods. Ellipsometry and infrared reflection−absorption spectroscopy confirmed that the cyclic peptide has horizontal orientation to the surface in the monolayer. Furthermore, absorption and fluorescence spectroscopy showed that the isolated electronic properties of the pyrene units are intact even in a condensed state in the monolayer.

## Introduction

Precise control of structures of molecules and their self-assemblies has been the central issue in chemistry.[1] It is important for clarification of operation principles in natural biological systems in which various molecules take regular shapes and are assembled into sophisticated structures.[2] It will also contribute to creation of novel molecular materials for electronics, photonics, and others in which functional molecules or their assemblies work at the molecular level.[3] One way to construct well-defined structures should be preparations of polygons and polyhedrons at the molecular level, which are actually common in nature and are essential for various biological functions. Recently, this type of chemistry has attracted much attention as "molecular architecture".[4] One of the main streams is coordination chemistry. Well-designed transition metals and multidentate organic ligands are spontaneously assembled into a well-defined structure. There have been extensive reports on molecular polygons, such as a triangle,[5] square,[6] and rectangle,[7] and molecular polyhedrons, such as a tetrahedron,[8] hexahedron,[9] and octahedron,[10] prepared by such metal coordination chemistry. Further assembling of these into

(1) Lehn, J. M. *Supramolecular Chemistry: Concepts and Perspectives*; VCH: Weinheim, Germany, 1995.
(2) (a) Beratan, D. N.; Onuchic, J. N.; Winkler, J. R.; Gray, H. B. *Science* **1992**, *258*, 1740−1741. (b) Wasielewski, M. R. *Chem. Rev.* **1992**, *92*, 435−461.
(3) (a) Aviram, A.; Ratner, M. A. *Chem. Phys. Lett.* **1974**, *29*, 277−283. (b) Carter, F. L. *Molecular Electronics Devices*; Dekker: New York, 1982. (c) Bumm, L. A.; Arnold, J. J.; Cygan, M. T.; Dunbar, T. D.; Burgin, T. P.; Jones, L.; Allara, D. L.; Tour, J. M.; Weiss, P. S. *Science* **1996**, *271*, 1705−1707. (d) Metzger, R. M.; Chen, B.; Hopfner, U.; Lakshmikantham, M. V.; Vuillaume, D.; Kawai, T.; Wu, X. L.; Tachibana, H.; Hughes, T. V.; Sakurai, H.; Baldwin, J. W.; Hosch, C.; Cava, M. P.; Brehmer, L.; Ashwell, G. J. *J. Am. Chem. Soc.* **1997**, *119*, 10455−10466. (e) Cui, X. D.; Primak, A.; Zarate, X.; Tomfohr, J.; Sankey, O. F.; Moore, A. L.; Moore, T. A.; Gust, D.; Harris, G.; Lindsay, S. M. *Science* **2001**, *294*, 571−574. (f) Donhauser, Z. J.; Mantooth, B. A.; Kelly, K. F.; Bumm, L. A.; Monnell, J. D.; Stapleton, J. J.; Price, D. W.; Rawlett, A. M.; Allara, D. L.; Tour, J. M.; Weiss, P. S. *Science* **2001**, *292*, 2303−2307. (g) Ramachandran, G. K.; Hopson, T. J.; Rawlett, A. M.; Nagahara, L. A.; Primak, A.; Lindsay, S. M. *Science* **2003**, *300*, 1413−1416.
(4) (a) Amabilino, D. B.; Stoddart, J. F. *Chem. Rev.* **1995**, *95*, 2725−2828. (b) Fujita, M.; Ogura, K. *Coord. Chem. Rev.* **1996**, *96*, 249−264. (c) Fyfe, M. C. T.; Stoddart, J. F. *Acc. Chem. Res.* **1997**, *30*, 393−401. (d) Navarro, J. A. R.; Lippert, B. *Coord. Chem. Rev.* **1999**, *186*, 653−667. (e) Tabellion, F. M.; Seidel, S. R.; Arif, A. M.; Stang, P. J. *J. Am. Chem. Soc.* **2001**, *123*, 7740−7741. (f) Kusukawa, T.; Fujita, M. *J. Am. Chem. Soc.* **2002**, *124*, 13576−13582. (g) Kryschenko, Y. K.; Seidel, S. R.; Muddiman, D. C.; Nepomuceno, A. I.; Stang, P. J. *J. Am. Chem. Soc.* **2003**, *125*, 9647−9652. (h) Nakabayashi, K.; Kawano, M.; Yoshizawa, M.; Ohkoshi, S.; Fujita, M. *J. Am. Chem. Soc.* **2004**, *126*, 16694−16695. (i) Tominaga, M.; Suzuki, K.; Murase, T.; Fujita, M. *J. Am. Chem. Soc.* **2005**, *127*, 11950−11951. (j) Yuan, Q. H.; Wan, L. J.; Jude, H.; Stang, P. J. *J. Am. Chem. Soc.* **2005**, *127*, 16279−16286.
(5) (a) Schnebeck, R. D.; Randaccio, L.; Zangrando, E.; Lippert, B. *Angew. Chem., Int. Ed.* **1998**, *37*, 119−121. (b) Sun, S. S.; Lees, A. J. *Inorg. Chem.* **1999**, *38*, 4181−4182. (c) Schnebeck, R. D.; Freisinger, E.; Glahe, F.; Lippert, B. *J. Am. Chem. Soc.* **2000**, *122*, 1381−1390.
(6) (a) Fujita, M.; Yazaki, J.; Ogura, K. *J. Am. Chem. Soc.* **1990**, *112*, 5645−5647. (b) Fujita, M.; Kwon, Y. J.; Washizu, S.; Ogura, K. *J. Am. Chem. Soc.* **1994**, *116*, 1151−1152. (c) Slone, R. V.; Yoon, D. I.; Calhoun, R. M.; Hupp, J. T. *J. Am. Chem. Soc.* **1995**, *117*, 11813−11814. (d) Stang, P. J.; Cao, D. H.; Saito, S.; Arif, A. M. *J. Am. Chem. Soc.* **1995**, *117*, 6273−6283. (e) Slone, R. V.; Hupp, J. T.; Stern, C. L.; AlbrechtSchmitt, T. E. *Inorg. Chem.* **1996**, *35*, 4096−4097.
(7) Kuehl, C. J.; Huang, S. D.; Stang, P. J. *J. Am. Chem. Soc.* **2001**, *123*, 9634−9641.
(8) Parac, T. N.; Caulder, D. L.; Raymond, K. N. *J. Am. Chem. Soc.* **1998**, *120*, 8003−8004.
(9) Takeda, N.; Umemoto, K.; Yamaguchi, K.; Fujita, M. *Nature* **1999**, *398*, 794−796.
(10) Olenyuk, B.; Whiteford, J. A.; Fechtenkotter, A.; Stang, P. J. *Nature* **1999**, *398*, 796−799.


**10.1021/ja061989d CCC: $33.50** 

higher-level structures has also been reported.[11] This methodology is very powerful for preparing highly symmetric structures from fewer kinds of components, but it is not very suitable for constructing asymmetric or chiral structures. Moreover, the uniformity and stability of the molecular assembly are sometimes of concern when the intended structure is one of multiple structures in equilibrium. The preparation conditions should thus be strictly optimized for quantitative and stable structure formation.

On the other hand, molecular architecture by covalent linkages will bear a precisely designed structure with few limitations but will be challenging. That is because syntheses of regularly shaped molecules are difficult and get much more difficult as the molecular sizes become larger. As is easily imagined, in the case of molecular polygons, for example cyclization of long, linear molecules should result in an extremely low yield because of low probability to cyclize. However, covalent methodology has many advantages such as allowance in the structure design, including asymmetric and chiral structures, and high uniformity and stability guaranteed by covalent linkages. These advantages should expand the potentials of molecular architecture. From our point of view, making a regular shape is not the goal of molecular architecture. It is important that the formed structure has functions unique to the structure and can be assembled into a higher-level well-defined structure. Therefore, rational molecular design using objective components is essential, and the components should be suitable not only to form the intended regular structure but also to provide the structure with functions and self-assembling properties. Thus far, we have focused our attention on helical peptides that are rigid and regular molecules with a wide allowance in the molecular design, intrinsic functions such as electron mediation due to the regularly arranged amide groups along the helix axis and electric-field generation due to their large dipole moment,[12] and an excellent ability to form regular self-assmblies.[13] As seen in nature, several peptide secondary structures including helices and sheets form sophisticated protein structures that are rational for their further self-assembling and their eventual functions. From this point of view, it is straightforward to use peptide secondary structures as well-defined components for molecular architecture. From reports of similar nature-inspired researches, molecular architectures using DNA duplexes such as a DNA triangle,[14] cube,[15] and octahedron[16] are well-known. However, molecular architecture using peptide secondary structures has been limited. As a unique example of peptide-based molecular architecture, we here demonstrate the covalent construction of a large molecular triangle from helical peptides. Although a triangle is the simplest form of polygons, there are few reports on exclusive molecular triangle formation even by the above-mentioned metal coordination techniques due to lack of ideal angular units to make the apex of 60°.[17] As for covalent molecular triangles, the examples are limited to just a few small molecules.[18]

Three linear components and three 60° angular components are needed to make a triangle. In the present work, a 9mer peptide having an alternative sequence of L-alanine (Ala) and α-aminoisobutyric acid (Aib) is chosen for the linear unit. It has been demonstrated that an 8mer Ala-Aib peptide takes $3_{10}$-helical conformation making one turn with three residues, whereas a 12mer Ala-Aib peptide takes α-helical conformation making one turn with 3.6 residues.[19] On the basis of this result, the 9mer peptide used in this study will take a $3_{10}$-helical structure. Assuming typical $3_{10}$-helical conformation with backbone dihedral angles, $\omega = 180°$, $\phi = -60°$, and $\psi = -30°$,[20] the terminal amino and carboxyl groups are located approximately on the same side of the helix in the case of 9mer peptides. This is suitable for making a regularly shaped triangle and is also one of the reasons why a 9mer peptide is chosen here. On the other hand, 8-aminopyrene-1-carboxylic acid (Pyr) is used for the angular unit. This unit has amino and carboxyl groups that are directly connected to the pyrene ring, and these functional groups protrude from the aromatic ring making a 60° angle between the two lines of the amino or carboxyl group and each connected carbon of the pyrene ring, that is ideal to make the apex of a triangle. The pyrene units are also used as a probe to investigate the molecular structure in this study. Furthermore, they can serve as a functional unit such as a photosensitizer or electron hopping site as mentioned in the Conclusion.

A linear 10mer peptide, Boc-Ala-Pyr-$(Ala\text{-}Aib)_4$-OMe, including the apex residue was synthesized as the repeating unit. The linear 30mer peptide, Boc-$[Ala\text{-}Pyr\text{-}(Ala\text{-}Aib)_4]_3$-OMe, was prepared by the repeated coupling of the 10mer units. Finally, after deprotection, the free ends were connected by a coupling reaction under a diluted condition to afford the cyclic peptide, cyclo$[Ala\text{-}Pyr\text{-}(Ala\text{-}Aib)_4]_3$ (Figure 1). It should be noted that this cyclic peptide is three-fold symmetric but lacks mirror symmetry, which is hard to construct by the conventional self-assembling techniques. We named it HT30 which is an abbreviation of a helix triangle composed of 30 amino acids.


(11) (a) Leininger, S.; Olenyuk, B.; Stang, P. J. *Chem. Rev.* **2000**, *100*, 853−907. (b) Fujita, M.; Umemoto, K.; Yoshizawa, M.; Fujita, N.; Kusukawa, T.; Biradha, K. *Chem. Commun.* **2001**, 509−518. (c) Holliday, B. J.; Mirkin, C. A. *Angew. Chem., Int. Ed.* **2001**, *40*, 2022−2043. (d) Qin, Z. Q.; Jennings, M. C.; Puddephatt, R. J. *Chem. Commun.* **2001**, 2676−2677.

(12) (a) Sisido, M.; Tanaka, R.; Inai, Y.; Imanishi, Y. *J. Am. Chem. Soc.* **1989**, *111*, 6790−6796. (b) Galoppini, E.; Fox, M. A. *J. Am. Chem. Soc.* **1996**, *118*, 2299−2300. (c) Fox, M. A.; Galoppini, E. *J. Am. Chem. Soc.* **1997**, *119*, 5277−5285. (d) Miura, Y.; Kimura, S.; Kobayashi, S.; Iwamoto, M.; Imanishi, Y.; Umemura, J. *Chem. Phys. Lett.* **1999**, *315*, 1−6. (e) Morita, T.; Kimura, S.; Kobayashi, S.; Imanishi, Y. *J. Am. Chem. Soc.* **2000**, *122*, 2850−2859. (f) Sisido, M.; Hoshino, S.; Kusano, H.; Kuragaki, M.; Makino, M.; Sasaki, H.; Smith, T. A.; Ghiggino, K. P. *J. Phys. Chem. B* **2001**, *105*, 10407−10415. (g) Morita, T.; Kimura, S. *J. Am. Chem. Soc.* **2003**, *125*, 8732−8733. (h) Kitagawa, K.; Morita, T.; Kimura, S. *J. Phys. Chem. B* **2004**, *108*, 15090−15095. (i) Yasutomi, S.; Morita, T.; Imanishi, Y.; Kimura, S. *Science* **2004**, *304*, 1944−1947. (j) Kitagawa, K.; Morita, T.; Kimura, S. *Angew. Chem., Int. Ed.* **2005**, *117*, 6488−6491. (k) Watanabe, J.; Morita, T.; Kimura, S. *J. Phys. Chem. B* **2005**, *109*, 14416−14425.

(13) (a) Fujita, K.; Kimura, S.; Imanishi, Y.; Okamura, E.; Umemura, J. *Langmuir* **1995**, *11*, 1675−1679. (b) Fujita, K.; Kimura, S.; Imanishi, Y.; Rump, E.; Ringsdorf, H. *Langmuir* **1995**, *11*, 253−258. (c) Miura, Y.; Kimura, S.; Imanishi, Y.; Umemura, J. *Langmuir* **1998**, *14*, 6935−6940. (d) Fujita, K.; Kimura, S.; Imanishi, Y. *Langmuir* **1999**, *15*, 4377−4379. (e) Kimura, S.; Kim, D. H.; Sugiyama, J.; Imanishi, Y. *Langmuir* **1999**, *15*, 4461−4463. (f) Miura, Y.; Kimura, S.; Imanishi, Y.; Umemura, J. *Langmuir* **1999**, *15*, 1155−1160. (g) Kimura, S.; Muraji, Y.; Sugiyama, J.; Fujita, K.; Imanishi, Y. *J. Colloid Interface Sci.* **2000**, *222*, 265−267. (h) Nishikawa, H.; Morita, T.; Sugiyama, J.; Kimura, S. *J. Colloid Interface Sci.* **2004**, *280*, 506−510. (i) Morino, N.; Kitagawa, K.; Morita, T.; Kimura, S. *Thin Solid Films* **2005**, *479*, 261−268. (j) Fukuda, M.; Sugiyama, J.; Morita, T.; Kimura, S. *Polymer J.* **2006**, *38*, 381−386.

(14) (a) Yang, X. P.; Wenzler, L. A.; Qi, J.; Li, X. J.; Seeman, N. C. *J. Am. Chem. Soc.* **1998**, *120*, 9779−9786. (b) Chelyapov, N.; Brun, Y.; Gopalkrishnan, M.; Reishus, D.; Shaw, B.; Adleman, L. *J. Am. Chem.* Soc. **2004**, *126*, 13924−13925. (c) Choi, J. S.; Kang, C. W.; Jung, K.; Yang, J. W.; Kim, Y. G.; Han, H. Y. *J. Am. Chem. Soc.* **2004**, *126*, 8606−8607.

(15) Chen, J. H.; Seeman, N. C. *Nature* **1991**, *350*, 631−633.

(16) Zhang, Y. W.; Seeman, N. C. *J. Am. Chem. Soc.* **1994**, *116*, 1661−1669.

(17) Kryschenko, Y. K.; Seidel, S. R.; Arif, A. M.; Stang, P. J. *J. Am. Chem. Soc.* **2003**, *125*, 5193−5198.

(18) (a) Pschirer, N. G.; Fu, W.; Adams, R. D.; Bunz, U. H. F. *Chem. Commun.* **2000**, 87−88. (b) Chadim, M.; Budesinsky, M.; Hodacova, J.; Zavada, J.; Junk, P. C. *Tetrahedron Asymmetry* **2001**, *12*, 127−133.

(19) Otoda, K.; Kitagawa, Y.; Kimura, S.; Imanishi, Y. *Biopolymers* **1993**, *33*, 1337−1345.

(20) Toniolo, C.; Benedetti, E. *Trends Biochem. Sci.* **1991**, *16*, 350−353.

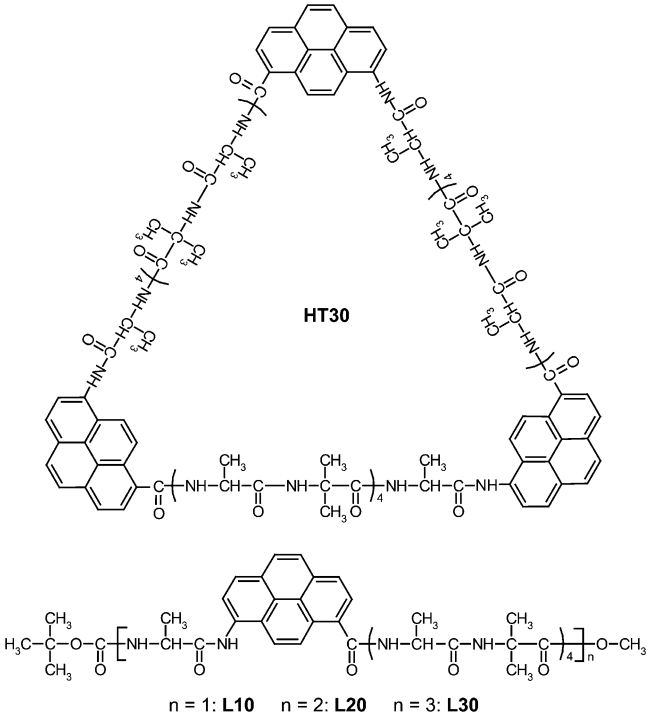


***Figure 1.*** Chemical structures of the helix triangle HT30 and the control linear peptides, L10, L20, and L30.

This unique cyclic peptide with a high molecular weight (MW = 2817.20) has many interesting prospects such as biological properties of a large cyclic peptide or a model ring protein, novel electronic functions or photofunctions taking advantage of the helical peptide units as well as the regularly located pyrene units, and abilities as well-defined building blocks to construct higher-level sophisticated assemblies.

The HT30 molecule was synthesized by the liquid-phase method, and the electronic properties of the pyrene units and the peptide conformation in solution were examined by absorption, fluorescence, and circular dichroism (CD) spectroscopies. In the spectroscopic analyses, the linear 10mer, 20mer, and 30mer peptides (L10, L20, L30; Figure 1), that are the synthetic intermediates of HT30, were used as control. On the basis of the spectroscopic results, the plausible molecular geometry was predicted by the semi-empirical molecular orbital method. To gain more information on the geometry and demonstrate one example of its self-assemblies, the monolayer of HT30 was prepared at the air/water interface and the surface pressure−area per molecule ($\pi$−$A$) isotherm was analyzed. The monolayer was then transferred onto a solid substrate, and the monolayer thickness, the molecular orientation, and the electronic properties of the pyrene units were investigated by ellipsometry, infrared reflection−absorption spectroscopy (IRRAS), and absorption and fluorescence spectroscopies.

## Results and Discussion

HT30 was synthesized by the cyclization reaction of the deblocked linear precursor (L30) using HATU and HOAt as coupling reagents. The details in the synthesis as well as the measurements and computational calculations are available in the Supporting Information. Despite the high molecular weight of the linear reactant (MW = 2835.22, L30 after deprotection), the reaction yield was relatively high (21.7%). As a reason for

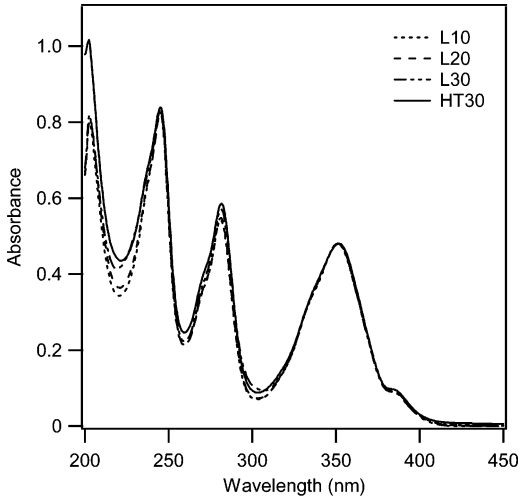


***Figure 2.*** Absorption spectra of L10, L20, L30, and HT30 in methanol measured at room temperature. The concentration of the pyrene unit = $2.0 \times 10^{-5}$ M.

that, it can be considered that the three pyrene units involved in the L30 molecule should bend the chain by 60° three times in one chain, which increases the encounter probability of the reactive terminals compared with that for the extended chain without the pyrene units. Furthermore, the electrostatic interaction between the terminals due to the positive and negative poles of the large dipole moment of the helical peptide in addition to the zwitterions of ammonium and carboxylate should stabilize the cyclic conformation of the chain. HT30 was identified by $^1$H NMR spectroscopy and two kinds of mass spectrometry, FAB and MALDI-TOF. To our best knowledge, HT30 (MW = 2817.20) is one of the highest molecular weight cyclic compounds with monodispersity ever synthesized without a vigorous process of fractionation if nucleic acids are excluded.[21]

The electronic properties of the pyrene units in HT30 were examined by absorption and fluorescence spectroscopy. Figure 2 shows the absorption spectra of HT30 and the reference linear peptides (L10, L20, and L30) recorded in methanol. A structural absorption pattern typical for pyrene derivatives with peaks at 245, 282, and 351 nm was observed. Due to its disubstituted nature, the absorption spectrum of the pyrene unit is broad and red-shifted compared to a spectrum of unsubstituted pyrene ($\lambda_{max}$ = 241, 275, 342 nm in methanol) with fine vibrational structures. All the spectra show nearly the same absorption pattern except for the slight difference perceived in the shorter wavelength. This result indicates that there is no electronic interaction between the three pyrene units in HT30 in the ground state. Figure 3 shows the fluorescence spectra of the peptides in methanol. Similarly to the absorption spectra, the fluorescence spectra also lack vibrational structures and are red-shifted compared to that of unsubstituted pyrene ($\lambda_{max}$ = 396 nm in methanol) due to the substitution effect. All the peptides show the same monomer emission at 446 nm, and their spectra are free from excimer emission at the longer wavelength. It should be noted that the emission intensity on the basis of one pyrene unit is not significantly reduced in HT30 compared to that of L10 having only one pyrene unit, despite the three pyrene units

(21) (a) Witherup, K. M.; Bogusky, M. J.; Anderson, P. S.; Ramjit, H.; Ransom, R. W.; Wood, T.; Sardana, M. *J. Nat. Prod.* **1994**, *57*, 1619−1625. (b) Daly, N. L.; Love, S.; Alewood, P. F.; Craik, D. J. *Biochemistry* **1999**, *38*, 10606−10614.

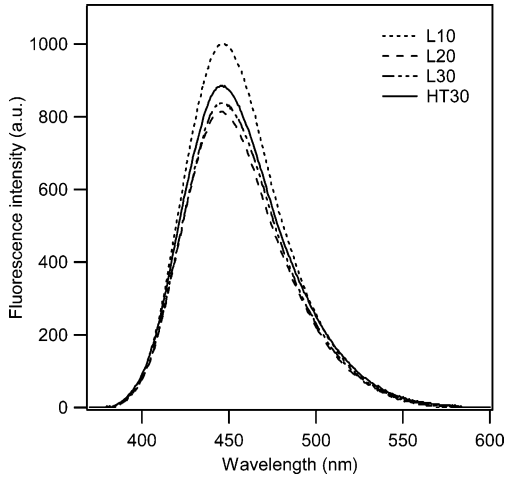


***Figure 3.*** Fluorescence spectra of L10, L20, L30, and HT30 in methanol measured at room temperature. The concentration of the pyrene unit was $2.0 \times 10^{-6}$ M, and the excitation wavelength is 350 nm.

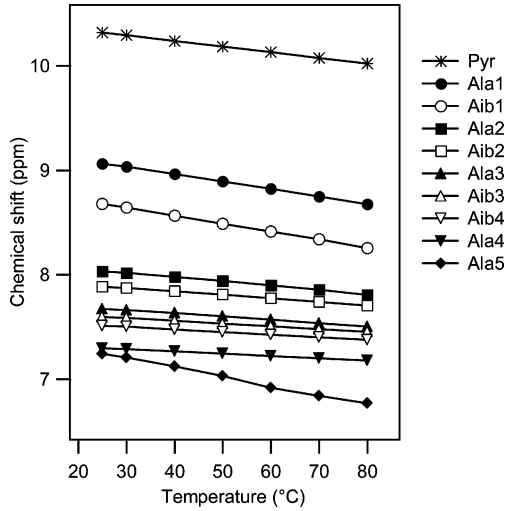


***Figure 4.*** Temperature dependence of the chemical shifts of the NH protons of L10 in deuterated dimethyl sulfoxide. Each of the Ala and Aib residues is numbered in order from the lower magnetic field.

being confined into one cyclic backbone. These observations clearly indicate that the pyrene units do not interact with each other in the excited-state either. According to these measurements, it is concluded that three pyrene units are separated from each other in the cyclic structure, in agreement with the aimed triangular structure.

Conformation of L10 in solution was analyzed by $^1$H NMR analysis. $^1$H NMR spectra of L10 in deuterated dimethyl sulfoxide were recorded at various temperatures, and the temperature dependence of the chemical shifts of the NH protons was analyzed (Figure 4). Each of Ala and Aib residues is numbered in the order from the lower magnetic field. It is well-known that an NH proton, free from hydrogen bonding and exposed to the solvent, changes its chemical shift as the temperature changes, whereas an NH proton forming a hydrogen bond keeps its chemical shift nearly unchanged against the temperature change.[22] In the case of $3_{10}$-helical conformation in which the carbonyl oxygen at *n* residue forms a bond with the amide proton at the *n*+3 residue, two NH protons at the N terminal are free from intramolecular bonding, whereas three

(22) Cierpicki, T.; Otlewski, J. *J. Biomol. NMR* **2001**, *21*, 249−261.

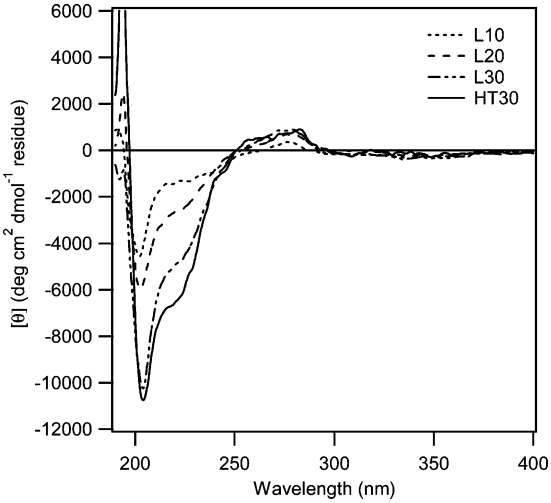


***Figure 5.*** CD spectra of L10, L20, L30, and HT30 in methanol measured at room temperature. The residue concentration ranged from $1.0 \times 10^{-4}$ to $2.0 \times 10^{-3}$ M.

NH protons are free from bonding in α-helical conformation in which the carbonyl oxygen at *n* residue forms a bond with the amide proton at the *n*+4 residue. Excluding the urethane NH proton of the Ala residue (Ala5) and the amide NH proton of the pyrene unit (Pyr) from the discussion due to the intermission of the pyrene residue, the chemical shifts of two amide NH protons (Ala1 and Aib1) significantly shift to the higher magnetic field with elevation of the temperature compared to the other NH protons, showing that L10 takes $3_{10}$-helical conformation in the sequence after the Pyr residue. Unfortunately, similar analyses for the other peptides were not performed due to the broadened nature of the NH region in their NMR spectra. For example, the NMR spectrum of HT30 in dimethyl sulfoxide showed broadened peaks, and further the sequence contains alternating Aib residues, which made precise assignments of the NH protons by 2D NMR measurements impractical.

Next, CD spectroscopy was performed to further investigate the peptide conformation in solution. The CD spectra of the peptides are shown in Figure 5. All the peptides showed a similar CD profile characterized by a sharp spike downward at 205 nm and the following broad shoulder at around 223 nm, that is typical for right-handed $3_{10}$-helical conformation.[23] This result indicates that the Ala-Aib sequence in each peptide takes $3_{10}$-helical conformation. Any significant exciton coupling between the pyrene units in HT30 did not appear in CD. The pyrene units are therefore well separated in the molecule, which is agreeable with the results of UV and fluorescence measurements. Interestingly, as the chain length of the linear peptide is elongated, the molar ellipticity increases especially from L20 to L30. This suggests that the helical conformation is stabilized by chain elongation that diminishes the effect of dangling terminals on the overall conformation even though the hydrogen bonds are not continuous at the pyrene units. As for L30, we speculate that the electrostatic attraction between the N and C terminals due to the large dipole of the helix should stabilize the overall cyclic structure close to a triangle, where the dangling motion of the terminals are suppressed to promote the helical

(23) Toniolo, C.; Polese, A.; Formaggio, F.; Crisma, M.; Kamphuis, J. *J. Am. Chem. Soc.* **1996**, *118*, 2744−2745.

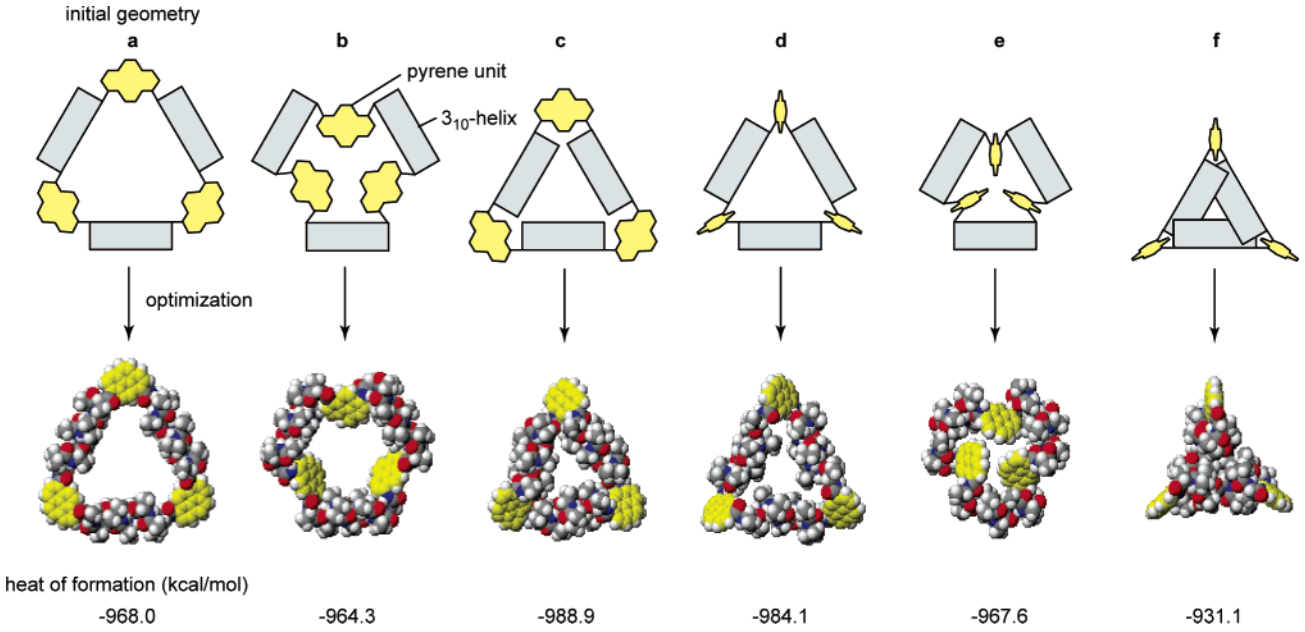


***Figure 6.*** Schematic presentations of the initial geometries used for computational geometry optimization (top) and the optimized geometries expressed in a space-filling model along with the respective heats of formation (bottom). The pyrene carbons are shown in yellow for clarity.

conformation. It is remarkable that HT30 retains a similar solid helical conformation guaranteed by the large molar ellipticity at 205 nm exceeding $-10000$ deg cm$^2$ dmol$^{-1}$ residue.[23] This finding indicates that the cyclization does not disturb the helical conformation, and that our molecular design is rational. Taken together, it is concluded that the three sides of the Ala-Aib sequence in HT30 takes a solid $3_{10}$-helical structure.

To obtain the plausible molecular structure of HT30, geometry optimization was carried out on computer. Three helical peptides and three pyrene units were manually linked to generate six different initial geometries as the representative probable geometries. They are schematically shown at the top of Figure 6. According to the CD spectroscopy, the typical dihedral angles of a $3_{10}$-helix ($\omega = 180°$, $\phi = -60°$, and $\psi = -30°$)[20] were used for the backbone of the helical peptide unit. In the geometries a−c, the axes of the helical peptide units are in the same plane, and the pyrene rings are parallel to the plane, whereas in the geometries d−f, the helix axes are inclined with each other and the orientation of the pyrene rings are vertical to the plane made of the three centers of the helical peptide units. These geometries were optimized by the Molecular Mechanics program 2 (MM2) method and the semi-empirical Austin Model 1 (AM1) method in this order to afford the respective final geometries with heat of formation (Figure 6 bottom). The initial geometry c afforded a triangular structure retaining perfect $3_{10}$-helical conformation with the lowest heat of formation ($-988.9$ kcal/mol), and the geometry d gave a similar structure with the second lowest energy ($-984.1$ kcal/mol). The other optimized geometries have higher formation energies compared to these two, and some of them are not triangular or do not hold $3_{10}$-helical conformation. These results demonstrate that the as-designed triangular structure, where the helical peptide units and the pyrene units make the sides and the apexes, respectively, is a stable and plausible structure for HT30. In the optimized geometry c with the lowest energy, as shown in Figure 7, the length of the triangle is 3.8 nm on a side, and the theoretical molecular area is calculated to be 6.3 nm$^2$, assuming trigonal arrangement of molecules and horizontal orientation on the two-dimensional plane. The cavity of the molecule also has a triangular shape with a 1.1 nm length on a side. As can be seen from the side view, the helix axes are slightly inclined from the molecular plane with a ca. 10° angle,

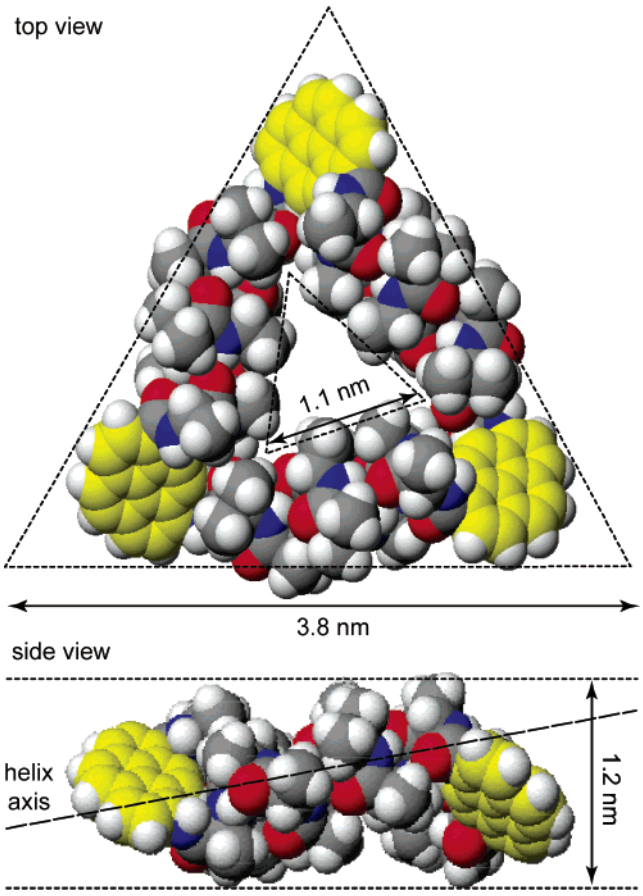


***Figure 7.*** Top view (top) and side view (bottom) of the optimized geometry c in a space-filling model. The pyrene carbons are shown in yellow for clarity.

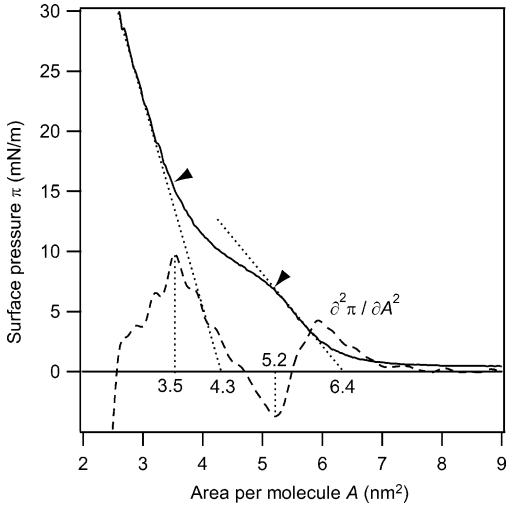


***Figure 8.*** $\pi-A$ isotherm of HT30 spread at the air/water interface (solid line) as well as its second-order derivative (dashed line) to determine the points of change (indicated by triangles). The measurement was performed with a compression rate of 5 $cm^2$/min at room temperature.

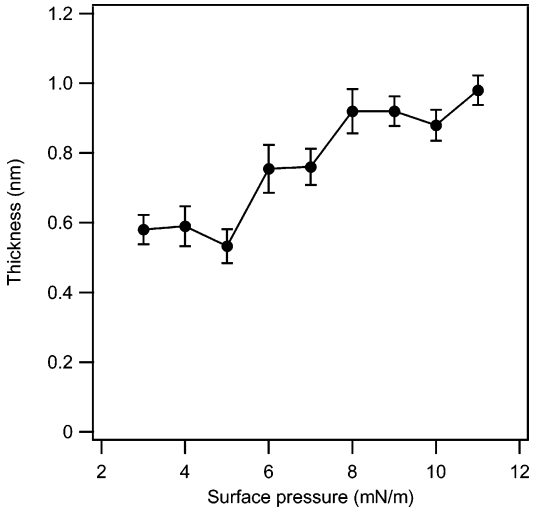


***Figure 9.*** Dependence of the thickness of the HT30 monolayer on gold measured by ellipsometry on the surface pressure set in the monolayer transfer.

and the pyrene rings also have a ca. 40° angle from the plane. The thickness of the molecule is 1.2 nm. For comparison with geometries of other peptide conformations, an α-helix and a fully extended chain were also analyzed. The initial geometries were generated in the same manner as the geometry c, and they were optimized similarly. The optimized geometries with α-helices and extended chains have heats of formation of −966.5 and −849.8 kcal/mol (data not shown), respectively, that are high compared with that of the optimized geometry c with $3_{10}$-helices. This clearly indicates the $3_{10}$-helix preference of the 9mer peptide units even confined into the cyclic structure and also agrees with the CD spectroscopy results. Summarizing these results, it is concluded that the triangular geometry with $3_{10}$-helices is plausible for the molecular structure of HT30.

To gain more information on the geometry as well as demonstrate one example of self-assembly composed of HT30, a monolayer of HT30 was prepared at the air/water interface. The trifluoroethanol solution of HT30 was spread on water, and the molecules were compressed at a constant rate. The $\pi-A$ isotherm is shown in Figure 8. The molecular area of HT30 was estimated from the extrapolation of the first linear region to zero surface pressure to be 6.4 $nm^2$, that is in a good agreement with that of the predicted geometries by computer (6.3 $nm^2$). It is thus considered that HT30 actually has a triangular structure similar to the predicted one and forms a well-packed monolayer in which the molecules are arranged in a trigonal manner with horizontal orientation to the water surface. Neighboring helical peptides in the monolayer would be stabilized by taking antiparallel orientation due to the favorable electrostatic interaction between their dipole moments, resulting in a nest arrangement of the triangles.

The first linear rise ends at 5.2 $nm^2$, and the second linear region starts at 3.5 $nm^2$. It is suggested that some change in orientation, arrangement, or conformation of the molecules occurs between these points of change to the final assembly form marked by a molecular area of 4.3 $nm^2$ (estimated by extrapolation of the second linear region).

To characterize the structure of the monolayer and examine the electronic properties of the pyrene units in the monolayer, the monolayer was transferred onto solid substrates by the vertical dipping method. A gold-coated glass substrate and quartz substrate were used for ellipsometry and infrared reflection−absorption spectroscopy (IRRAS), and absorption and fluorescence spectroscopies, respectively. Preliminary experiments showed that the monolayer transfer at downstroke was incomplete, whereas the transfer at the upstroke was nearly quantitative. The transfer was thus done only at the upstroke to avoid disordering the monolayer. The thicknesses of the monolayers transferred on gold at various surface pressures were measured by ellipsometry. The relationship between the thickness and the surface pressure is shown in Figure 9. The thicknesses of the monolayers transferred at surface pressures <6 mN/m are much smaller than that of the predicted geometry, assuming horizontal orientation (1.2 nm). This suggests that the monolayer was not quantitatively transferred due to insufficient surface pressure. On the other hand, the thickness rapidly increases across the surface pressure of 6−7 mN/m and stays constant again, 0.9 nm on average. The transfer ratios at the surface pressures >7 mN/m were 1.1−1.2, suggesting quantitative monolayer transfer. The thickness of 0.9 nm by ellipsometry is slightly thinner than that of 1.2 nm by calculation (Figure 7). Since ellipsometry evaluates the average thickness of the monolayer, correction should be carried out for the monolayer of HT30 having the molecular cavity. Taking the cavity of HT30 into account, the apparent molecular thickness is calculated to be 1.0−1.1 nm, which is close to the observed value.

The substrates were subjected to IRRAS measurement to evaluate the molecular orientation. The IRRAS spectrum of the monolayer transferred at 9 mN/m is shown in Figure 10. Amide I and amide II were observed at 1669 and 1539 $cm^{-1}$, respectively. The tilt angle of the helix axis from the surface normal was calculated on the basis of the absorbance ratio of amides I and II. Figure 11 shows the dependence of the tilt angle of the helix axis on the surface pressure set in the monolayer transfer. Tilt angles are almost independent of the surface pressure and are 70−75°. The angles of helix axes from the surface are thus 15−20°. Assuming horizontal orientation with the molecular plane parallel to the surface, these angles agree with the predicted geometry because the helix axes in the geometry have a ca. 10° angle from the molecular plane (Figure 7 bottom). On the basis of these results, it is found that

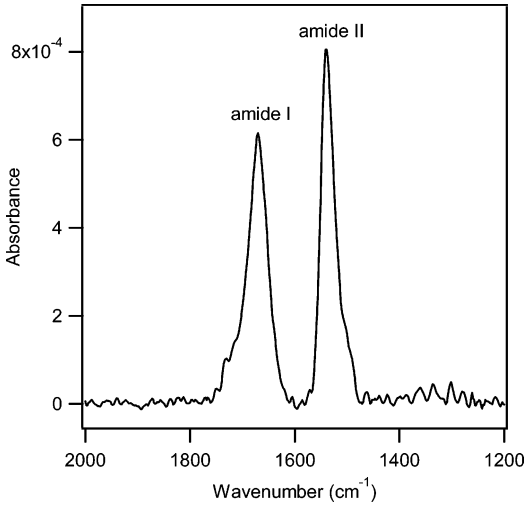


***Figure 10.*** IRRAS spectrum of the HT30 monolayer transferred on gold at the surface pressure of 9 mN/m.

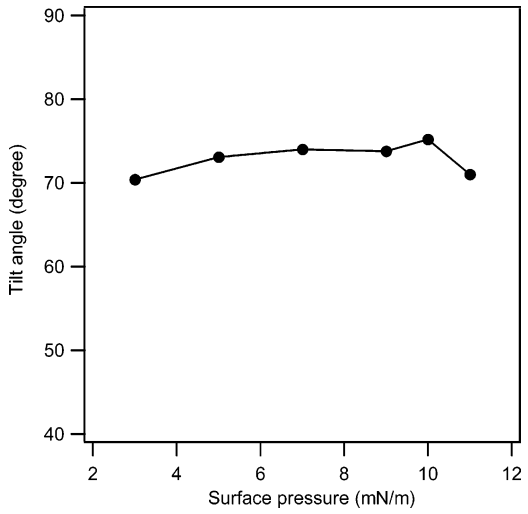


***Figure 11.*** Relationship between the tilt angle of the helix axis in the HT30 monolayer and the surface pressure set in the monolayer transfer. The tilt angles were determined on the basis of the absorbance ratio of the amide I and amide II.

a monolayer of the triangular molecules with trigonal packing and horizontal orientation to the surface is successfully prepared on a gold substrate by transferring the monolayer at surface pressure between 8 and 11 mN/m.

Further, the monolayer transferred on quartz at surface pressure of 9 mN/m was studied by absorption and fluorescence measurements (Figure 12). Absorption and fluorescence spectra were similar to those in solution. The pyrene unit in the monolayer is therefore isolated intramolecularly and intermolecularly from surrounding pyrene units in terms of the electronic structures despite the highly condensed state in the monolayer. We infer from this finding regularity and rigidity of the HT30 molecule. From the absorbance at 351 nm in the absorption spectrum, the molecular area was calculated to be 5.3 $nm^2$, that is relatively close to the molecular areas estimated by the geometry optimization (6.3 $nm^2$) and the $\pi-A$ isotherm (6.4 $nm^2$), suggesting that a well-packed monolayer with horizontal orientation should be formed on the quartz substrate. The slight disagreement in the molecular areas is probably due to the surface roughness of the quartz substrate used. The surface of solid substrates generally has irregularity and thus can accommodate a larger number of molecules per the apparent area than the flat water surface.

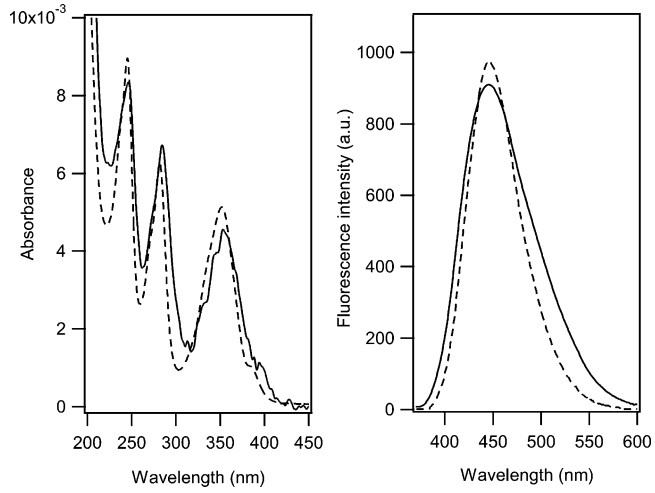


***Figure 12.*** Absorption (left) and fluorescence (right) spectra of the HT30 monolayer transferred on a quartz substrate at the surface pressure of 9 mN/m (solid lines), together with the respective spectra in solution (dashed lines). The excitation wavelength of the fluorescence spectroscopy is 350 nm.

On the basis of these measurements of the monolayers, it is finally concluded that the HT30 molecule has a triangle structure similar to that predicted by the geometry optimization, that it forms a stable monolayer at the air/water interface with trigonal arrangement and horizontal orientation to the surface, and that the monolayer can be quantitatively transferred onto solid substrates with preservation of the molecular structure and orientation.

## Conclusion and Future Plans

In this study, as a unique example of peptide-based molecular architecture, a large-sized triangular molecule, what we call a helix triangle, was constructed with a relatively high yield by using specifically designed building blocks of three $3_{10}$-helical peptides and three pyrene units. Various spectroscopic measurements of HT30 in solution and on substrates as well as isotherm analysis of its monolayer and computational calculations revealed that the helix triangle actually has a triangular structure composed of the $3_{10}$-helical peptide units as the sides and the pyrene units as the apexes, and that the helix-triangle molecules form a stable well-packed monolayer with trigonal arrangement and horizontal orientation to the surface at the air/water interface. The monolayer can also be transferred onto solid substrates with preservation of the molecular and monolayer structures. As mentioned briefly in the Introduction, this helix triangle has significant potential in many ways. First of all, it is one of the highest molecular weight cyclic compounds with monodispersity and is the largest covalent molecular triangle ever synthesized. At the same time, it is one of the largest cyclic peptides, whether natural or artificial, and is the first example of a cyclic peptide containing helices in its backbone. Cyclic peptides have been extensively studied as biologically active substances as well as useful models for protein structures and functions.[24] Moreover, considering its large size and symmetric shape with a regular cavity, the helix triangle is reminiscent of ring protein structures that are commonly found in DNA polymerases, DNA helicases, and chaperonins.[25] It is thus interesting to investigate how this

large cyclic peptide interacts with biological molecules. In preliminary studies, inclusion of small-chain molecules by the helix triangle cavity is now being investigated. Second, its photoelectronic and electrochemical behaviors are appealing. It has been reported that helical peptides mediate electron-transfer reactions better than saturated compounds due to the regularly arranged amide groups, and the dipole moment of the helical peptides accelerates electron transfer in the same direction as that of the dipole moment due to the electric field generated by the dipole moment. In the case of the helix triangle, it is interesting that the three helical peptide units are arranged in a head−tail fashion in terms of the dipole moment direction. Therefore, when a cation radical of the pyrene unit is generated by laser irradiation or electrochemical redox reactions, the radical ion can circularly hop among the pyrene units in one direction according to the dipole moment, possibly generating a magnetic field in the direction normal to the molecular plane. Such a molecular electromagnet has never been explored. To examine such a potential, transient absorption spectroscopy by laser flash photolysis is in progress. Third, helical peptides have an intrinsic property to form regular self-assemblies as seen in natural protein structures. Taking advantage of this property, it is possible to design and prepare various types of unique self-assemblies. As demonstrated in this study, a monolayer in which the helix triangles are laterally arranged to cover the two-dimensional surface is one of them. Not only that, a nanotube in which the helix triangles are stacked on each other in the direction normal to the molecular plane can also be designed. This tubular assembly is interesting for its potential as a catalyst, a size-selective encapsulating host, a transportation channel for small molecules, and a molecular solenoid, regarding the above-mentioned molecular electromagnet. Investigation on such nanotube formation is also under way.

**Acknowledgment.** This work is partly supported by Grant-in-Aids for Young Scientists B (16750098), for Exploratory Research (17655098), and for Scientific Research B (15350068), and 21st century COE program, COE for a United Approach to New Materials Science, from the Ministry of Education, Culture, Sports, Science, and Technology, Japan.

**Supporting Information Available:** Details of the syntheses, monolayer preparation, spectroscopic measurements in solution and of the monolayers, and computational calculations. This material is available free of charge via the Internet at http://pubs.acs.org.

JA061989D

(24) (a) Ovchinnikov, Y. A.; Ivanov, V. T. *Tetrahedron* **1975**, *31*, 2177−2209. (b) Kessler, H. *Angew. Chem., Int. Ed. Engl.* **1982**, *21*, 512−523. (c) Ghadiri, M. R.; Granja, J. R.; Milligan, R. A.; McRee, D. E.; Khazanovich, N. *Nature* **1993**, *366*, 324−327. (d) Rao, A. V. R.; Gurjar, M. K.; Reddy, K. L.; Rao, A. S. *Chem. Rev.* **1995**, *95*, 2135−2167. (e) Seebach, D.; Matthews, J. L.; Meden, A.; Wessels, T.; Baerlocher, C.; McCusker, L. B. *Helv.* Chim. Acta **1997**, *80*, 173−182. (f) Clark, T. D.; Buehler, L. K.; Ghadiri, M. R. *J. Am. Chem. Soc.* **1998**, *120*, 651−656. (g) Ranganathan, D.; Haridas, V.; Gilardi, R.; Karle, I. L. *J. Am. Chem. Soc.* **1998**, *120*, 10793−10800. (h) Ranganathan, D.; Haridas, V.; Karle, I. L. *J. Am. Chem. Soc.* **1998**, *120*, 2695−2702. (i) Ranganathan, D.; Lakshmi, C.; Karle, I. L. *J. Am. Chem. Soc.* **1999**, *121*, 6103−6107. (j) Lambert, J. N.; Mitchell, J. P.; Roberts, K. D. *J. Chem. Soc., Perkin Trans. 1* **2001**, 471−484.

(25) (a) Kelman, Z.; Finkelstein, J.; Odonnell, M. *Curr. Biol.* **1995**, *5*, 1239−1242. (b) Fenton, W. A.; Horwich, A. L. *Protein Sci.* **1997**, *6*, 743−760.